PAPER 11

LONG-TERM INFILTRATION MEASUREMENTS IN A FULL-SCALE TEST STRUCTURE

M.P. MODERA, M.H. SHERMAN, D.T. GRIMSRUD
Lawrence Berkeley Laboratory, USA

INTRODUCTION

Researchers, for some time, have been working on the problems of measurement and modeling of infiltration in residential structures. Basic research, however, has been hampered by the lack of long-term data from a fully-instrumented, full-scale structure. The Mobile Infiltration Test Unit (MITU) was designed and built at the Lawrence Berkeley Laboratory (LBL) to meet such a need. MITU spent the 1980-1981 winter in the field collecting the data required for infiltration modeling. This data includes: measured infiltration rates, surface pressures, wind velocities, indoor and outdoor temperatures, leakage area and leakage distribution.

Analysis of the MITU data has allowed us to, (1) evaluate models of envelope leakage using surface pressure and infiltration data, and (2) evaluate a model which uses the concept of effective leakage area, along with weather data, to predict infiltration rates.

MITU TRAILER

MITU[1] is a commercially available construction-site office trailer that was modified and instrumented by researchers at LBL. Illustrated in Figure 1, MITU is a portable self-contained test structure designed to perform extended infiltration field studies in a variety of climates, allowing complete control of building parameters and site parameters. It is instrumented to provide for validation of both long-term average and hour-by-hour infiltration-model predictions. The trailer is also designed to test various components of the model individually (i.e., translation of airport wind data into wind at the structure, reduction of wind-induced pressures due to localized shielding, etc.).

MITU is a wood-frame structure, 4.9 meters (16 ft) long, 2.4 meters (8 ft) wide, and 2.4 meters (8 ft) high. It contains both heating and cooling systems and requires only electrical power from each site. The walls and floor of the trailer contain a total of sixteen window openings that can be fitted with interchangeable calibrated leakage panels for controlling total leakage, leakage distribution, and leakage type (i.e., narrow cracks, large holes). The trailer shell is sealed with a continuous vapor barrier, and perforations are caulked with silicone sealant to minimize the leakage. The leakage of the panels and the trailer shell are determined with a specially designed fan pressurization system that fits into one of the window openings and measures air flow using an orifice plate.

Air infiltration, weather data, and surface pressures are sampled, reduced, and recorded on floppy disk by a Z-80 microprocessor-based computer.

This work was funded by the Assistant Secretary for Conservation and Renewable Resources, Office of Buildings and Community Systems, Buildings Division of the U.S. Department of Energy under contract No. W-7405-Eng-48.

Air infiltration is monitored with the Continuous Infiltration Monitoring System (CIMS) developed at LBL.[2] This system computes and stores half-hour average infiltration rates.

Windspeed and wind direction are measured at two heights, 5.5 meters (18 ft) and 10 meters (33 ft) above the ground. The sensors are mounted on collapsible weather towers that are permanently affixed to the rear of the trailer. Outdoor temperature is monitored by a sensor mounted 7 meters (23 ft) above the ground. Speeds, directions and temperatures are checked every 10 seconds and recorded on disk as half hour averages.

Surface pressures from 82 taps located on the walls, floor and ceiling are measured with differential pressure transducers. Taps are opened and closed by computer-controlled solenoid valves. During sampling, each tap is kept open for ten seconds. The pressure signal, sampled 40 times per second, is electronically filtered using a one-second time constant in order to eliminate any ringing in the pressure lines due to solenoid operation. The pressures are monitored with pressure transducers on six levels. Four of the transducers are on the walls at 0.23m (0.75 ft), 0.90m (2.95 ft), 1.57m (5.15 ft) and 2.24m (7.35 ft) above the floor of the trailer, while the remaining two transducers are for the ceiling and floor. All pressures, including inside pressure (measured with an additional transducer), are measured relative to a pressure reservoir that communicates with indoor pressure with a two minute time constant. This system allows for direct measurement of stack-induced pressures and the height of the neutral level. The zero of each transducer is checked every thirty minutes and subtracted from the surface pressures, which are then stored as thirty-minute averages.

LEAKAGE MODELS

The most important factor for determining natural infiltration is the resistance of the building shell to air flow. The flow resistance, or leakage, is measured with a technique known as fan pressurization. This involves pressurizing and depressurizing the structure to known pressure differences and measuring the resulting flow response. In order to determine the curve relating the pressure drop across the envelope to the flow that it induces, the flows at each pressure differential are plotted on log-log paper. In the pressure region used (10 to 60 Pa) the data generally form a straight line; i.e., the data are well represented by the empirical (power fit) relationship:

$$Q = K \Delta P^n \qquad (1)$$

where

- Q is the volume flow rate of the fan [m^3/s],
- K is a constant,
- ΔP is the absolute value of the pressure drop across the building envelope [Pa] , and
- n is an exponent in the range $0.5 < n < 1.0$.

Researchers at LBL characterize the flow resistance of the cracks and openings in the building shell in terms of the effective leakage area. The concept of effective leakage area approximates flow resistance using square-root flow; i.e., it assumes that the flow through the apertures in the building shell is similar to orifice flow, where the flow rate is proportional to the square root of the pressure drop across the opening. This implies that the flow through the building shell can be represented by:

$$Q = L \sqrt{\frac{2}{\rho} \Delta P} \qquad (2)$$

where

ΔP is the pressure drop across the building shell [Pa],
L is the effective leakage area [m^2], and
ρ is the density of air [kg/m^3].

To use fan pressurization data to determine leakage area, the flows in Equations 1 and 2 are equated at a reference pressure:

$$L = K \sqrt{\frac{\rho}{2}} (\Delta P_r)^{n - \frac{1}{2}} \qquad (3)$$

where

K is the graphically determined constant,
L is the effective leakage area [m^2],
ρ is the density of air [kg/m^3], and
ΔP_r is the reference pressure [Pa].

The reference pressure we have chosen, 4 Pa, is typical of weather-induced, infiltration-driving pressures.

MITU FIELD TRIP

The Mobile Infiltration Test Unit was stationed in Reno, Nevada for the past winter (December, 1980 - March, 1981). The site was chosen for its low temperatures, high winds, and lack of shielding from the wind (see Figure 1). During the four-month period, data was collected under a variety of conditions; the quantity, shape and distribution of leakage area were varied, as well as the orientation of the trailer on the site.

INFILTRATION FROM SURFACE PRESSURES

The measured infiltration rates and surface pressure data collected during the MITU field trip can be used to compare the hypothesis of square-root flow to the more exact power-fit leakage model. Since the location and flow characteristics of all of the leakage sites are known, measured surface pressures can be used to predict the flows in and out of the trailer shell. We made these predictions using our square-root flow leakage model (see Equation 2), and using the power fit leakage model (Equation 1) with a flow exponent of 0.65. A flow exponent of 0.65 was chosen for two reasons: the measured flow exponents for the leakage panels were between 0.6 and 0.7; additionally, 0.65 is the quoted flow exponent in many leakage studies. Figures 2 and 3 are plots of measured infiltration, infiltration predicted by square-root flow

(n= 0.5), and infiltration predicted with a 0.65 flow exponent. The flows are calculated assuming a normal (Gaussian) pressure distribution over time, using measured mean pressures and standard deviations. Infiltration is determined by integrating flow times the probability density function between zero and positive infinity, while exfiltration is determined by integrating between negative infinity and zero. The plotted curves represent the average of predicted infiltration and predicted exfiltration. In Figure 2, both square-root and power fit predictions track measured infiltration quite well. As one might expect, the flows predicted with a flow exponent of 0.65 exceed square-root flows at high infiltration rates (high pressure differences), and are lower than square-root predictions at low infiltration rates (low pressure differences). In general, at pressure differences below 4 Pa (the pressure at which leakage area is determined), square-root flows will be higher, while above 4 Pa, power fit (n=0.65) flows will be higher. Despite these differences, the square-root and power fit models give very similar results over the course of the test. Although square-root and power-fit predictions show good agreement in Figure 3, they both underpredict considerably during the high infiltration periods near the end of the test. A possible explanation is suggested when one examines a plot of wind direction over the course of the test. During the entire period of underprediction, the wind direction varies between thirty degrees east and thirty degrees west of north. Wind tunnel studies of pressure coefficients on structures with similar aspect ratios have shown that for winds from these angles, the pressure coefficients change sign as one proceeds along the east and west faces.[3] Since the measurement system physically averages the pressures across a given face, it will sum positive pressures with negative pressures, resulting in an underprediction of pressures and therefore flows.

Although they should agree, the average predicted infiltration and exfiltration disagreed by as much as 25% for many data sets. One cause could be an offset in the measured pressure differences, possibly caused by stack effects in the vertical lines connecting the pressure reservoir to the pressure transducers. By adding a uniform pressure offset to the measured pressures it was found that a 0.1 to 0.3 Pa offset (corresponding to a few degrees C temperature difference) resulted in flow equalization for all data sets. Although the difference between infiltration and exfiltration was significantly affected by the pressure offset, the average value did not change.

INFILTRATION MODEL

A residential infiltration model has been developed at LBL[4,5] using the concept of effective leakage area. It uses building and site parameters to make infiltration predictions from available weather data. The model was specifically designed for simplicity; that is, precise detail was sacrificed for ease of application. The functional form of the model, along with some important assumptions, is presented below.

The basic form of the infiltration model is:

$$Q = L \sqrt{f_s^2 \Delta T + f_w^2 v^2} \qquad (4)$$

where

Q is the infiltration [m^3/s],
L is the effective leakage area [m^2],
ΔT is the indoor-outdoor temperature difference [K],
f_s is the stack parameter [$m/s/K^{1/2}$],
v is the wind speed, and
f_w is the wind parameter.

In this expression, f_w and f_s, the wind and stack parameters, essentially convert the wind speed, v, and the indoor-outdoor temperature difference, ΔT, into equivalent pressures across the leakage area of the house. The terms inside the square root actually have the units of velocity squared, i.e., pressure over density. The wind and stack parameters are weather independent quantities that depend upon the distribution of leakage area, the degree to which the house is shielded from the wind, and some geometrical parameters.

INFILTRATION MODEL VALIDATION

Half-hour average infiltration predictions were made for 34 days of data from the MITU field trip, using weather data and appropriate values for each of the model parameters. A compact method of displaying this large data set is with a histogram of the ratio of predicted-to-measured infiltration; Figure 4 shows the distribution of this ratio. Although this plot shows a symmetric (log-normal) distribution about the mean, it also indicates that the average ratio of half-hour infiltration predictions to the measured infiltration rates is 1.23. Although one would like the data to be centered about unity, this mean ratio does not imply that the average predicted infiltration will be 23% high. A histogram of ratios weights all infiltration rates equally, implying that a systematic error at low infiltration rates, although small in absolute value, will have a large effect on the mean ratio. The average predicted infiltration for this data set (1600 measurements) was 34.4 m^3/hr, while the average measured infiltration was 32.5 m^3/hr.

Although the histogram is useful for presenting the entire set, a plot of measured and predicted infiltration against time provides information about the tracking ability of the model. Figure 5 is a plot of air infiltration rate vs. time for a three-day period and Figure 6 displays the results of a four-day test using a different leakage configuration. In both figures, the model predictions track measured infiltration quite well. Although the infiltration rate changes by a factor of ten over the course of the four-day test, the model falls short only at some of the higher infiltration rates. Both plots show a slight overprediction at lower infiltration rates. These results encourage using the model to provide short-term infiltration predictions in situations that require hour-by-hour infiltration measurements, e.g., measurement of the thermal characteristics of buildings, indoor air quality tests, etc.

The data sets plotted in Figures 5 and 6 correspond to the same dates as Figures 2 and 3, respectively. Comparing Figures 2 and 5, the average flow rate predicted by the infiltration model agrees remarkably well with the square-root flow prediction from measured pressure differences. A comparison of Figures 3 and 6

reveals some interesting discrepancies. At high infiltration rates, the infiltration model tracks the measured flow rate quite well, yet both square-root and power fit flows underpredict considerably. The close agreement of infiltration model predictions with measured infiltration rates supports the earlier hypothesis of pressure measurement system inaccuracies as the cause of these underpredictions.

CONCLUSIONS

The Mobile Infiltration Test Unit has been an excellent source of field data, allowing us to carefully examine the problems associated with infiltration in residential structures. Comparisons of measured infiltration rates with values calculated from surface pressures have shown no decrease in accuracy when a square-root flow model is used instead of the general power-fit model of leakage. We therefore conclude that the square-root flow leakage model is preferable to a power-fit model, because of its direct physical interpretation.

The measurement results have clearly demonstrated that great care must be taken when making surface pressure measurements: temporal and spatial pressure averaging can lead to significant errors in infiltration predictions. Additionally, very small temperature differences in the pressure measurement system can cause large apparent disagreements between infiltration and exfiltration. Combining these difficulties with the successful predictions of the LBL infiltration model, we conclude that the determination of infiltration from surface pressures has provided both a validation of the LBL model, as well as a justification for the use of predictive infiltration models.

REFERENCES

1. Blomsterberg, A. K., Modera, M.P., Grimsrud, D.T.. 1981. The mobile infiltration test unit-- Its design and capabilities: Preliminary experimental results. Lawrence Berkeley Laboratory report, LBL-12259.

2. Sherman, M. H., Grimsrud, D. T., Smith, B. V.. 1980. Air infiltration measurement techniques. Proc. of the 1st AIC Conf., London.

3. Bowen, A. J.. 1976. A wind tunnel investigation using simple building models to obtain mean surface wind pressure coefficients for air infiltration estimates. Nat. Research Council, Canada, Nat. Aero. Estab. Tech. Rep. LPR-LA-209.

4. Sherman, M.H.. 1981. Air infiltration in buildings. (Lawrence Berkeley Laboratory report, LBL-10712).

5. Sherman, M.H., Grimsrud, D.T.. 1980. The measurement of infiltration using fan pressurization and weather data. Proc. of 1st AIC Conf., London.

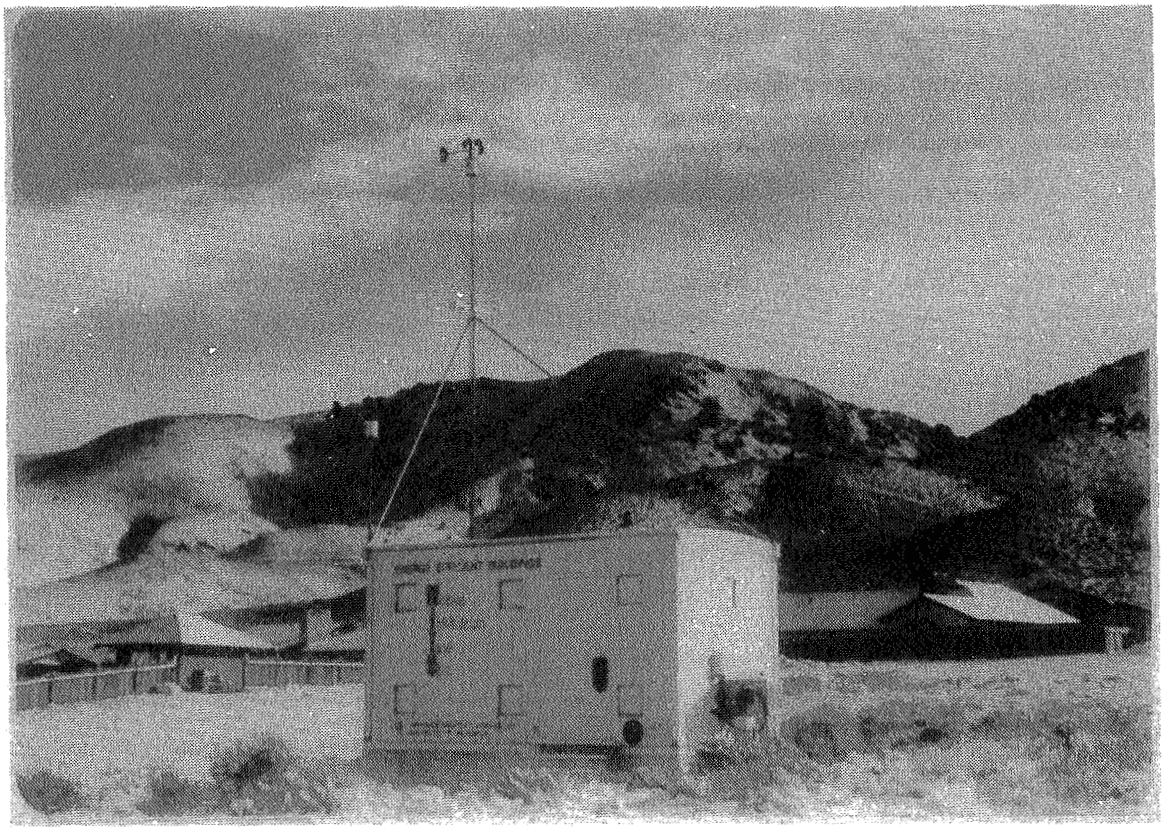

Figure 1. Mobile Infiltration Test Unit in Reno, Nevada test site.

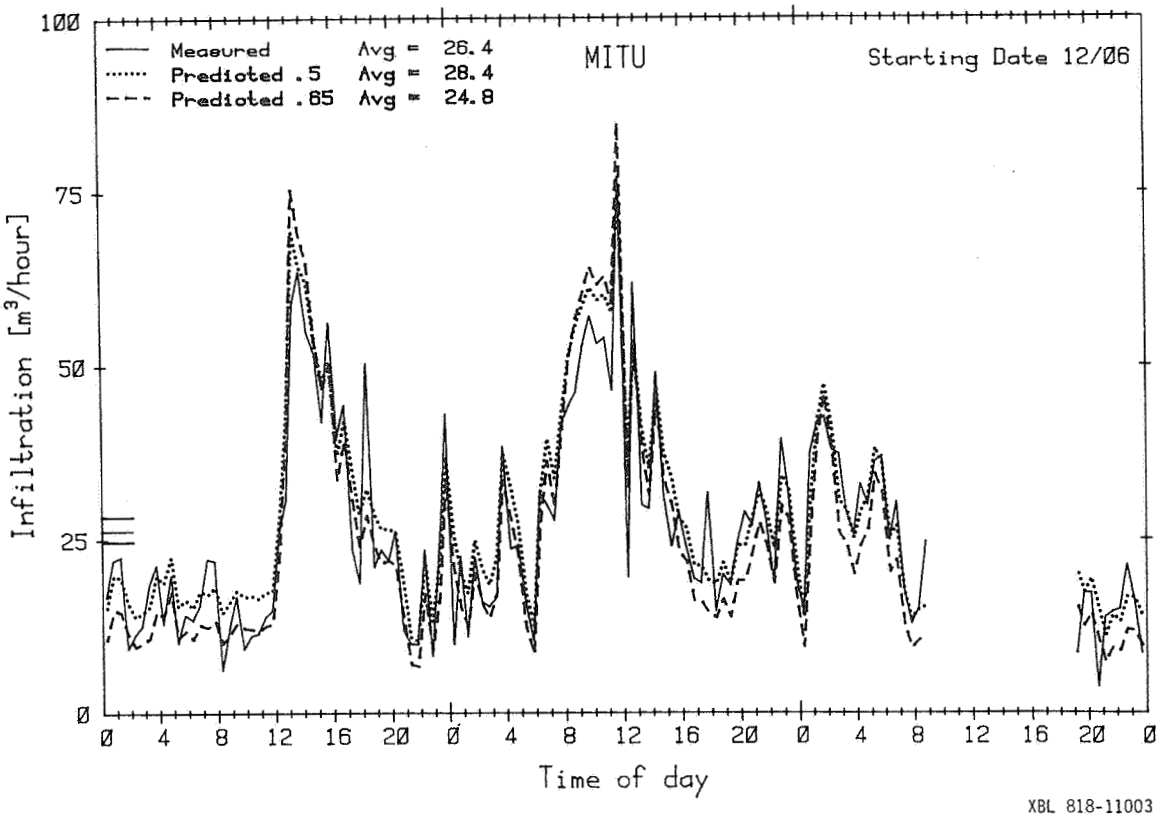

Figure 2. Plot of measured infiltration and infiltration predictions from surface pressures vs. time: Three-day test in MITU.

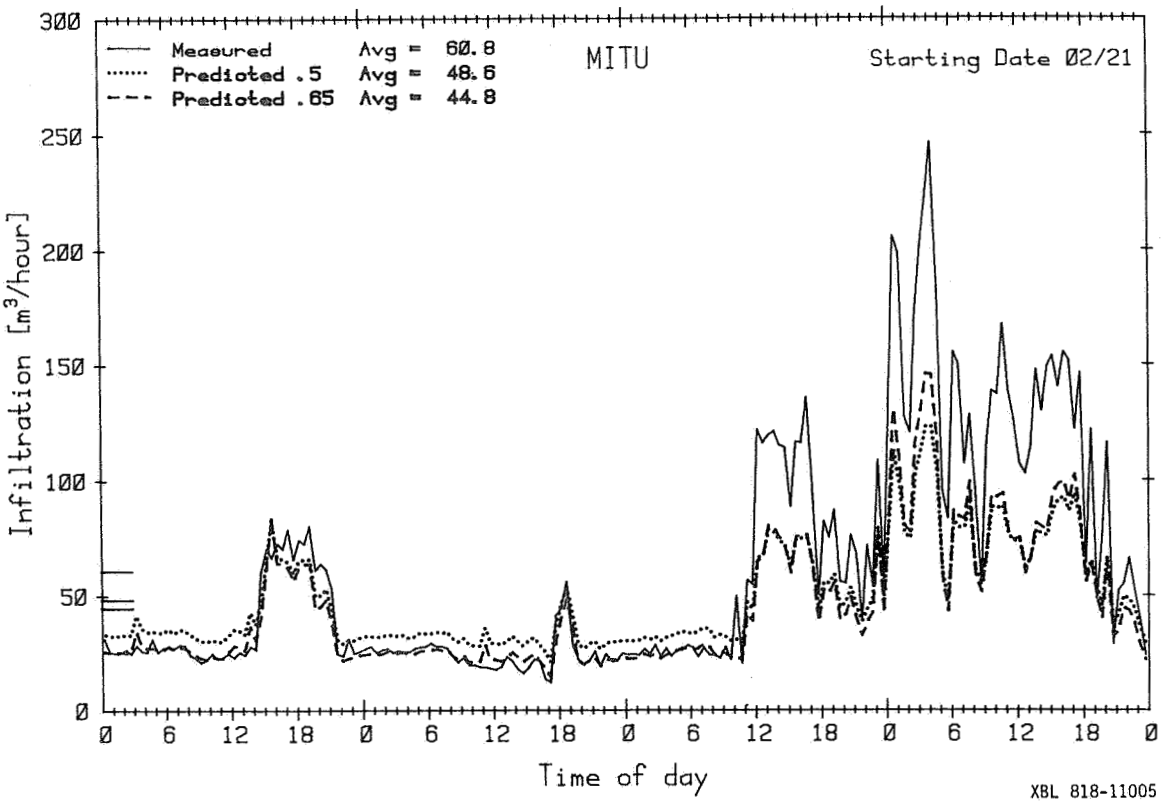

Figure 3. Plot of measured infiltration and infiltration predictions from surface pressures vs. time: Four-day test in MITU.

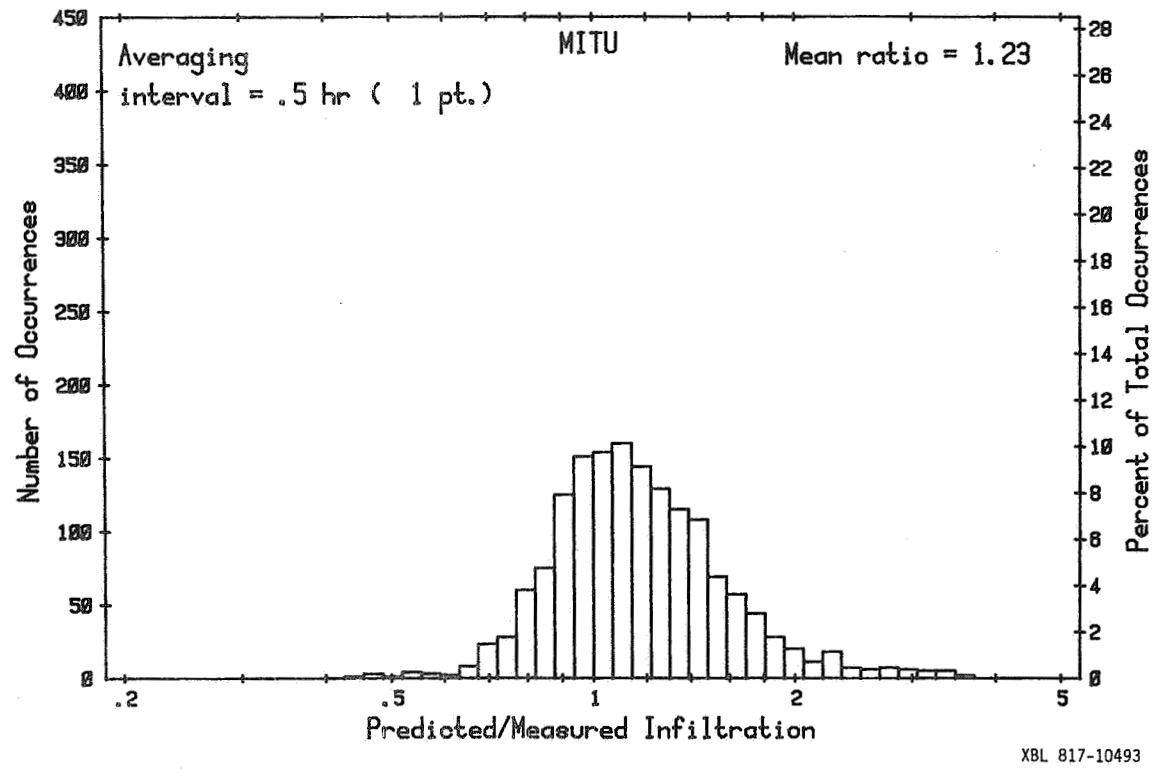

Figure 4. Histogram of predicted infiltration/measured infiltration for 34 days of data from MITU.

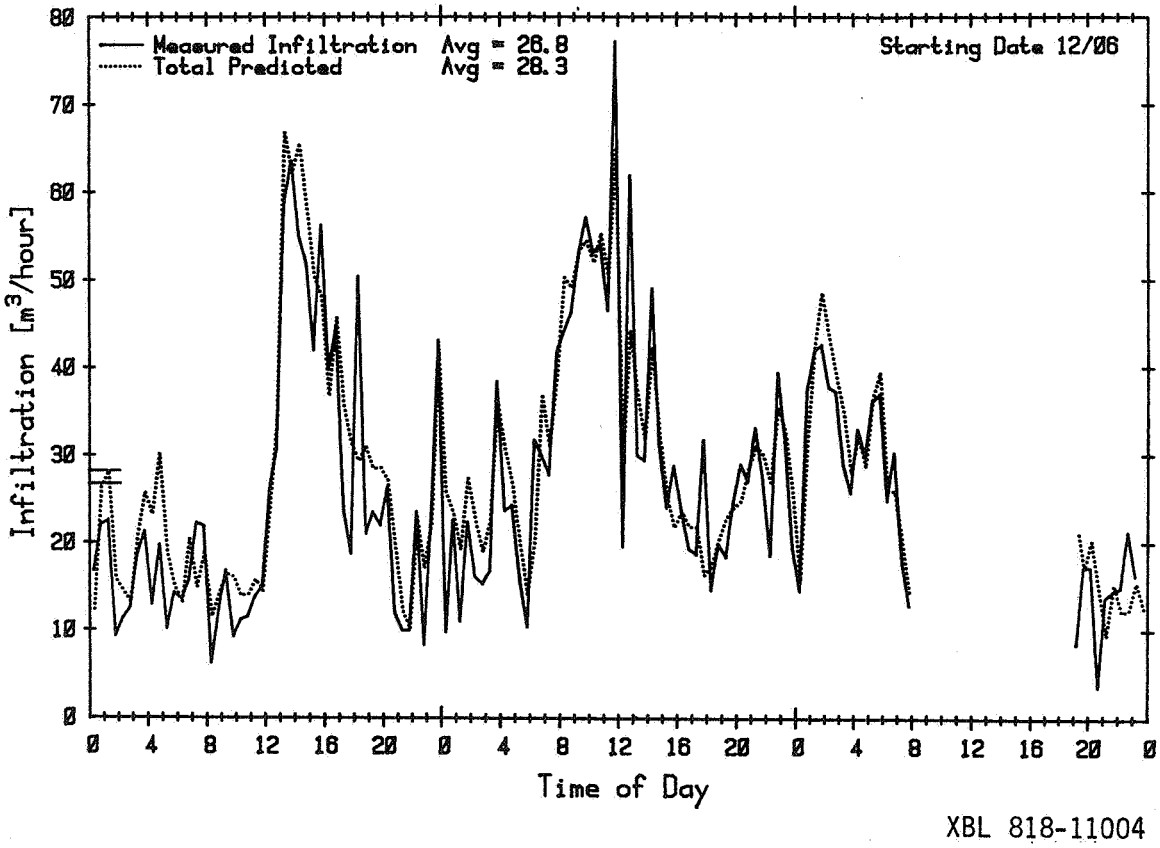

Figure 5. Plot of measured infiltration and infiltration model predictions vs. time: Three-day test in MITU.

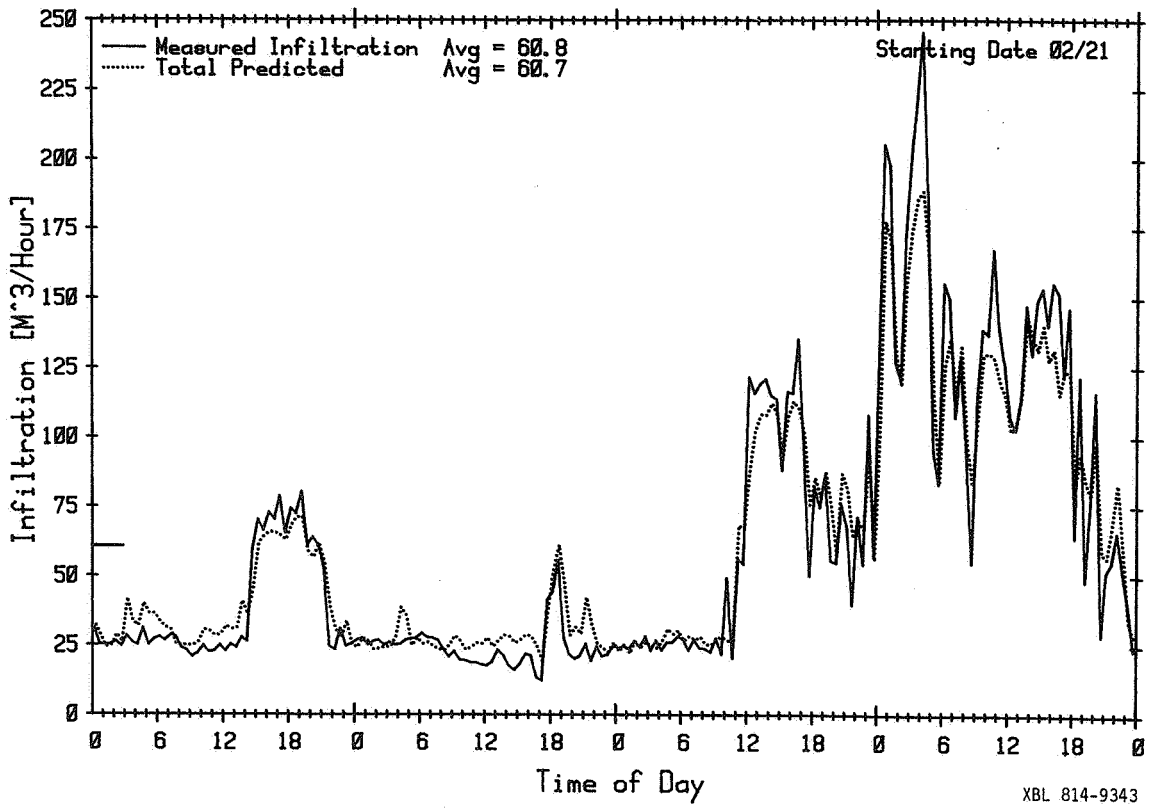

Figure 6. Plot of measured infiltration and infiltration model predictions vs. time: Four-day test in MITU.